IEEE Access
Multidisciplinary | Rapid Review | Open Access Journal

Date of publication xxxx 00, 0000, date of current version xxxx 00, 0000.

Digital Object Identifier 10.1109/ACCESS.2017.DOI

Improved Schemes of Differential Spatial Modulation

RUEY-YI WEI[1], (Senior Member, IEEE), YI-WEI TSAI[2], and SHIH-LUN CHEN[1]

[1]Department of Communication Engineering, National Central University, Taoyuan, Taiwan, R.O.C.
[2]National Chung-Shan Institute of Science & Technology, Taoyuan, Taiwan, R.O.C.

Corresponding author: Ruey-Yi Wei (e-mail: rywei@ncu.edu.tw)

ABSTRACT Differential spatial modulation (DSM) is able to transmit additional data bits without increasing radio-frequency circuits and power consumption and also avoids pilot overhead. In this paper, we propose two new schemes of DSM to improve the original DSM. One is an increased-rate scheme that transmits one additional data bit per two blocks. The bit mapping and maximum-likelihood detection is particularly designed. The other scheme is to increase the diversity of DSM. By properly designing block coded modulation and complex antenna-index matrices, the proposed scheme can achieve the desired diversity order. Compared with the existing schemes with the same constellation of the transmitted signals, the proposed scheme achieves higher transmission rates.

INDEX TERMS spatial modulation, block coded modulation, differential encoding

I. INTRODUCTION

Various multi-antenna techniques have been proposed for increasing transmission rates of wireless communications. Among them, spatial modulation (SM) [1]- [4] which uses a single transmit antenna each time attracts much attention. Compared with the conventional single-antenna system, SM is able to transmit additional data bits by selecting indexes of antennas without increasing RF circuits and power consumption.

The original SM technique is coherent and thus is not suitable for rapidly-varying channels. For such channels, differential SM (DSM) [5], [6] together with differential detection can avoid pilot overhead. In fact, DSM is a special case of differential space-time modulation (DSTM) [13], [14]. Original DSM and DSTM use the same encoding and decoding process, but DSM activates single transmit antenna each time while DSTM does not have such restriction. DSM with complex-valued antenna-index matrices in [6] has better error performance than DSM in [5] whose entries of antenna-index matrices are 0 and 1. However, the complex-valued matrices are obtained through random searches in [6], and there are unlimited possibilities of transmitted signals after differential encoding. In [7], we proposed a systematic design of complex-valued antenna-index matrices to avoid the unbounded constellation size.

In this paper, we propose two improved schemes of DSM. One scheme is increased-rate DSM which transmits one additional data bit per two blocks. In each transmitted block, the number of permutating the antenna index is not a power of two, so some permutations are not mapped by data bits. By utilizing the unused permutations of two blocks, one additional data bit can be transmitted. Adding bits on modulation, e.g, from QPSK to 8PSK, decreases the minimum Euclidean distance in the signal space, so the error probability increases significantly. However, adding bits in permutation does not affect the minimum Euclidean distance in the signal space, so the error probability increases very slightly. The permutations of two blocks have to be detected jointly, which increases the detection complexity exponentially. Therefore, we propose a simpler maximum-likelihood (ML) detection method instead, which increases the detection complexity linearly. Besides, we also consider bit mapping which affects bit error rates. In addition to a conventional mapping method, we propose a new bit-mapping method that uses a look-up table. Both theoretical analysis and computer simulations show that this new bit mapping outperforms the conventional one.

The other scheme is increased-diversity DSM. The DSMs in [5] and [7] are full-rate, i.e., there is no redundancy for increasing diversity. To increase diversity, DSM using repeated symbols was proposed in [6], and various coded DSM schemes were designed in [9]- [12]. In this paper,

This article has been accepted for publication in a future issue of this journal, but has not been fully edited. Content may change prior to final publication. Citation information: DOI 10.1109/ACCESS.2021.3095531, IEEE Access

we propose a different method to increase the diversity of DSM. The proposed scheme called block coded DSM (BC-DSM) utilizes coherent multilevel block coded modulation (BCM) [16], [17] to encode nonzero symbols. By properly designing complex antenna-index matrices and BCM, the desired diversity order can be achieved. Compared with coded DSM schemes in [6] and [9]- [12] with the same signal constellation, BC-DSM has higher data rates. In other words, to the authors' best knowledge, BC-DSM is the most bandwidth-efficient coded DSM scheme given a fixed MPSK (M-ary phase-shift keying) constellation of the transmitted signals.

The remainder of this paper is organized as follows. In Sec. II, we first review DSM and BCM, and slightly modify the complex-valued antenna-index matrices in [7]. In Sec. III, we propose the increased-rate DSM scheme including simplified ML detection and bit-mapping methods. Then we propose BC-DSM scheme including an algorithm which searches antenna-index matrices for a desired diversity in Sec. IV. Finally Sec. V concludes this paper.

Notation: $(.)^\dagger$, $\|.\|$ and rank$(.)$ denote the conjugate transpose, the Frobenius norm and the rank of a matrix, respectively. diag$\{.\}$ represents the operation from a row vector to a diagonal matrix. $\lfloor\rfloor$ denotes the floor function. $\mathcal{CN}(0,\sigma^2)$ denotes the zero-mean, σ^2-variance, complex Gaussian distribution.

II. PRELIMINARIES

Consider a communication system with N_T transmitter antennas and N_R receiver antennas. The channels between antenna pairs are Rayleigh-fading and independent of each other. Each block of DSM contains N_T time slots. For the tth block, the transmitted signal is represented by an $N_T \times N_T$ matrix $\mathbf{S}(t)$, and there is only one nonzero entry in each column and row of $\mathbf{S}(t)$. For the tth block, the $N_R \times N_T$ matrix of received signals is

$$\mathbf{Y}(t) = \mathbf{H}(t)\mathbf{S}(t) + \mathbf{N}(t) \tag{1}$$

where $\mathbf{H}(t)$ is the $N_R \times N_T$ matrix of channel coefficients whose entries are $\mathcal{CN}(0,1)$, and $\mathbf{N}(t)$ is the $N_R \times N_T$ matrix of AWGN with $\mathcal{CN}(0, N_0)$ entries.

The number of permutating the antenna index is $N_T!$, but only $L = 2^{\lfloor \log_2 N_T! \rfloor}$ permutations are used. For the tth block, $\log_2 L$ bits determine an antenna-index matrix $\mathbf{A}(t) \in \mathcal{A} = \{\mathbf{A}_0, \mathbf{A}_1, \cdots, \mathbf{A}_{L-1}\}$ and other data bits decide N_T symbols $\mathbf{x}(t) = [x_1(t), x_2(t), \cdots, x_{N_T}(t)] \in \mathcal{X}$ where $\mathcal{X}$ denotes the set of all possible values of $\mathbf{x}(t)$. At the transmitter, $\mathbf{S}(t)$ is determined by

$$\mathbf{S}(t) = \mathbf{S}(t-1)\mathbf{X}(t). \tag{2}$$

where $\mathbf{X}(t)$ is an $N_T \times N_T$ data matrix calculated by

$$\mathbf{X}(t) = \text{diag}\{\mathbf{x}(t)\}\mathbf{A}(t). \tag{3}$$

At the receiver, the noncoherent maximum-likelihood (ML) detection is

$$\hat{\mathbf{X}}(t) = \arg \min_{\tilde{\mathbf{X}} \in \mathcal{X}'} \|\mathbf{Y}(t) - \mathbf{Y}(t-1)\tilde{\mathbf{X}}\|^2 \tag{4}$$

where $\mathcal{X}'$ denotes the set of all possible values of $\mathbf{X}(t)$. For any two different elements in $\mathcal{X}'$, denoted by $\mathbf{X}$ and $\mathbf{X}'$, the minimum value of rank$(\mathbf{X}-\mathbf{X}')$ which represents transmitter diversity order, denoted by d_T, should be maximized first [14].

The low-complexity noncoherent ML detector proposed in [7] is described as follows. Let $p_l^{(k)}$ represent the position of the nonzero entry, $e^{j\theta_{l,k}}$, in the kth column of $\mathbf{A}_l$ where $k \in \{1, 2, \cdots, N_T\}$ and $l \in \{0, 1, \cdots, L-1\}$. At the receiver, $\forall l \in \{0, 1, \cdots, L-1\}$, the determined $\mathbf{x}(t)$ for $\mathbf{A}_l$, denoted by $\hat{\mathbf{x}}_l(t) = [\hat{x}_1^{(l)}(t), \hat{x}_2^{(l)}(t), \cdots, \hat{x}_{N_T}^{(l)}(t)]$, are obtained by

$$\hat{x}^{(l)}_{p_l^{(k)}}(t) = \arg \min_{\tilde{x}} \sum_{i=1}^{N_R} |y_{ik}(t) - y_{ip_l^{(k)}}(t-1)\tilde{x}e^{j\theta_{l,k}}|^2 \tag{5}$$

and the metric of $\mathbf{A}_l$ is

$$m_l(t) = \sum_{k=1}^{N_T}\sum_{i=1}^{N_R} |y_{ik}(t) - y_{ip_l^{(k)}}(t-1)\hat{x}^{(l)}_{p_l^{(k)}}(t)e^{j\theta_{l,k}}|^2. \tag{6}$$

The detected value of $\mathbf{A}(t)$ is $\mathbf{A}_{\hat{l}}$ satisfying

$$\hat{l} = \arg \min_{l \in \{0,1,\cdots,L-1\}} m_l(t) \tag{7}$$

and the detected value of $\mathbf{x}(t)$ is

$$\hat{\mathbf{x}}(t) = \hat{\mathbf{x}}_{\hat{l}}(t). \tag{8}$$

The signal constellation of the elements in $\mathbf{x}(t)$ is M-ary PSK where $M = 2^b$ and b is an integer. For the full-rate DSM [5]- [7], the number of data bits mapped to $\mathbf{x}(t)$ is $N_T b$, so the spectral efficiency is $\frac{\log_2 L}{N_T} + b$ bits/s/Hz. In [7], by a systematic construction for $\mathcal{A}$, the diversity between any two different antenna-index matrices is increased. However, due to uncoded data symbols $\mathbf{x}(t)$, the overall transmitter diversity of the full-rate DSM is still only one.

Consider be the systematic construction proposed in [7]. In this $\mathcal{A}$, there are only two types of $\mathbf{A}(t)$: the nonzero entries are all 1, or all $e^{j\theta}$. We have shown in [7] that if two matrices in this $\mathcal{A}$ have only two different elements of the permutation order, then the two matrices belonging to two different types and the transmitter diversity between them is N_T. Take $N_T = 4$ as an example: for $\mathbf{A} = \begin{pmatrix} 1 & 0 & 0 & 0 \\ 0 & 1 & 0 & 0 \\ 0 & 0 & 1 & 0 \\ 0 & 0 & 0 & 1 \end{pmatrix}$ and $\mathbf{A}' = \begin{pmatrix} 0 & 1 & 0 & 0 \\ 1 & 0 & 0 & 0 \\ 0 & 0 & 1 & 0 \\ 0 & 0 & 0 & 1 \end{pmatrix}$, rank$(\mathbf{A}-\mathbf{A}')$ is only 1, so $\mathbf{A}'$ in the construction in [7] becomes $\mathbf{A}' = \begin{pmatrix} 0 & e^{j\theta} & 0 & 0 \\ e^{j\theta} & 0 & 0 & 0 \\ 0 & 0 & e^{j\theta} & 0 \\ 0 & 0 & 0 & e^{j\theta} \end{pmatrix}$ such that rank$(\mathbf{A}-\mathbf{A}')$ becomes 4. In [7], the optimal value of θ is obtained by considering such $\mathbf{A}$ and $\mathbf{A}'$ where the rank of $\mathbf{A}-\mathbf{A}'$ is full. However, there exist two different matrices belong to the same type, and the transmitter diversity between

This article has been accepted for publication in a future issue of this journal, but has not been fully edited. Content may change prior to final publication. Citation information: DOI 10.1109/ACCESS.2021.3095531, IEEE Access

them is only two, e.g., $\mathbf{A}$ and $\mathbf{A}'' = \begin{pmatrix} 0 & 1 & 0 & 0 \\ 0 & 0 & 1 & 0 \\ 1 & 0 & 0 & 0 \\ 0 & 0 & 0 & 1 \end{pmatrix}$. To calculate the coding gain, only codeword-pairs with the least diversity are considered. Therefore, the value of θ is independent of the coding gain which is based on codeword-pairs with $d_T = 2$ such as $(\mathbf{A}, \mathbf{A}'')$. To minimize the number of the points in the signal constellation for $\mathbf{S}(t)$, we choose $\theta = \frac{\pi}{M}$ in this paper. By doing so, the signal constellation of $\mathbf{S}(t)$ is only $2M$-ary PSK.

A short description for BCM using M-ary PSK is given as follows. For the convenience of presentation, we restrict M to 8. Consider 8PSK whose signal points are labeled by three bits (a, b, c), where a, b, and $c \in \{0, 1\}$. Let $(a_1, b_1, c_1), (a_2, b_2, c_2), \cdots, (a_{N_T}, b_{N_T}, c_{N_T})$ be a block of transmitted 8PSK signals with length N_T. A multilevel block-coded 8PSK C is designed in such a manner that $\mathbf{c_a} = (a_1, a_2, \cdots, a_{N_T})$ is a codeword of a binary block code C_a, $\mathbf{c_b} = (b_1, b_2, \cdots, b_{N_T})$ is a codeword of a binary block code C_b and $\mathbf{c_c} = (c_1, c_2, \cdots, c_{N_T})$ is a codeword of a binary block code C_c. Herein, C_i represents the component code used for coding level i, where $i \in \{a, b, c\}$. The transmitted codeword of C composed of $\mathbf{c_a}, \mathbf{c_b}$ and $\mathbf{c_c}$ is $\mathbf{x} = \exp\{j\frac{2\pi}{M}(\mathbf{c_a} + 2\mathbf{c_b} + 4\mathbf{c_c})\}$.

Assume that C_i is an (N_T, k_i, d_i) binary block code, where d_i denotes the minimum Hamming distance of C_i for $i \in \{a, b, c\}$. Each block consists of N_T 8PSK signals and the data rate is $(k_a + k_b + k_c)/N_T$ bits per 8PSK signal. The minimum Hamming distance of C, i.e., the minimum value of distinct symbols between two different codewords in C, is $\min\{d_a, d_b, d_c\}$. In this letter, in order to maximize data rates given a minimum Hamming distance, we use Gray labeling and choose $d_a = d_b = d_c$, i.e., component codes $C_a = C_b = C_c$.

III. INCREASED-RATE DSM

Let $\mathcal{A}' = \{\mathbf{A}_0, \mathbf{A}_1, \cdots, \mathbf{A}_{N_T!-1}\}$ denote the set of all possible antenna-index matrices. If $N_T!^2 \geq 2L^2$ which is true for $N_T = 3, 4, 5$, then the total permutations of the antenna index in two blocks is enough to transmit $2\log_2 L+1$ data bits. We propose two methods to map $2\log_2 L + 1$ data bits to $\mathbf{A}(t-1)$ and $\mathbf{A}(t)$.

A. A SIMPLE BIT MAPPING METHOD

This bit mapping is straightforward and is similar to the bit mapping in [8]. For the $t-1$th and tth blocks, $2\log_2 L + 1$ data bits form an integer m $(0 \leq m < 2L^2)$ first. Dividing m by $N_T!$ gives out a quotient of q with a remainder of r. The antenna-index matrices $\mathbf{A}(t-1)$ and $\mathbf{A}(t)$ are $\mathbf{A}_q$ and $\mathbf{A}_r$, respectively. Let $2L^2 - 1$ (the largest value of m) divided by $N_T!$ gives out a quotient of q' with a remainder of r'. The set of possible values of (q, r), denoted by Ω, is $\{(0,0), (0,1), (0,2), \cdots, (0, N_T!-1), (1,0), (1,1), \cdots, (1, N_T!-1), \cdots, (q', r')\}$.

Throughout this section, $\mathbf{A}_{\hat{q}}$ and $\mathbf{A}_{\hat{r}}$ denote the detected values of $\mathbf{A}(t-1)$ and $\mathbf{A}(t)$ at the receiver, respectively. The value of m is estimated by

$$\hat{m} = \hat{q} \times N_T! + \hat{r} \tag{9}$$

and the $2\log_2 L + 1$ detected data bits are generated accordingly. However, $\mathbf{A}_{\hat{q}}$ and $\mathbf{A}_{\hat{r}}$ cannot be separately determined because there are $(N_T!)^2 - 2L^2$ unused pairs of $(\mathbf{A}(t-1), \mathbf{A}(t))$. The noncoherent ML detection is

$$(\hat{q}, \hat{r}) = \arg \min_{(l,l') \in \Omega} m_l(t-1) + m_{l'}(t) \tag{10}$$

where $m_l(t)$ is the metric of $\mathbf{A}_l$ of the tth block defined in (6). Note that performing (10) has to try all $2L^2$ possible values of (l, l') in Ω.

We propose a simplified ML detection method which first finds

$$\tilde{q} = \arg \min_{l \in \{0,1,\cdots,q'-1\}} m_l(t-1) \tag{11}$$

$$\tilde{r} = \arg \min_{l' \in \{0,1,\cdots,N_T!-1\}} m_{l'}(t). \tag{12}$$

and

$$\tilde{l}' = \arg \min_{l' \in \{0,1,\cdots,r'\}} m_{l'}(t). \tag{13}$$

and then $\mathbf{A}_{\hat{q}}$ and $\mathbf{A}_{\hat{r}}$ are determined by (14) shown on the next page.

The comparison of metrics in (14) is easy, so the main complexity of the proposed detection is the minimization in (11)-(13). The minimization in (13) can be obtained during the minimization in (12), so to obtain $\tilde{q}$, $\tilde{r}$, and $\tilde{l}'$, only $q' + N_T! < 2N_T!$ values are tested, which is less than the complexity of performing (10). Before compare the complexity between (10) and (14) by examples, we first show that the proposed detection is ML detection.

Theorem 1: The detection by (14) is equivalent to the noncoherent ML detection by (10).

Proof: There are two cases for $(\hat{q}, \hat{r})$ in (10): (i) $\hat{q} \in \{0, 1, \cdots, q'-1\}$ and $\hat{r} \in \{0, 1, \cdots, N_T!-1\}$; (ii) $\hat{q} = q'$ and $\hat{r} \in \{0, 1, \cdots, r'\}$. For case (i), $(\tilde{q}, \tilde{r})$ has the lowest metric $m_{\tilde{q}}(t-1) + m_{\tilde{r}}(t)$ in (10), so we have $\hat{q} = \tilde{q}$ and $\hat{r} = \tilde{r}$ and $m_{\tilde{q}}(t-1) + m_{\tilde{r}}(t) < m_{q'}(t-1) + m_{\tilde{l}'}(t)$; while for case (ii), $(q', \tilde{l}')$ has the lowest metric $m_{q'}(t-1) + m_{\tilde{l}'}(t)$ in (10), so we have $\hat{q} = q'$ and $\hat{r} = \tilde{l}'$ and $m_{\tilde{q}}(t-1) + m_{\tilde{r}}(t) > m_{q'}(t-1) + m_{\tilde{l}'}(t)$. □

Example 1: For $N_T = 3$, the number of the permutations of the antenna index in one block is $3! = 6$, so the original DSM has $L = 4$ and the spectral efficiency 2.667 bits/s/Hz for $M = 4$. In the proposed scheme, we use 5 data bits to choose 32 antenna indexes from all $6 \times 6 = 36$ permutations, so the spectral efficiency becomes 2.833 bits/s/Hz for $M = 4$. Because $q' = 5$ and $r' = 1$ $(31 = 6 \times 5 + 1)$, the used matrices of $(\mathbf{A}(t-1), \mathbf{A}(t))$ are $(\mathbf{A}_0, \mathbf{A}_0)$,$(\mathbf{A}_0, \mathbf{A}_1)$,$\cdots$,$(\mathbf{A}_0, \mathbf{A}_5)$,$(\mathbf{A}_1, \mathbf{A}_0)$,$\cdots$,$(\mathbf{A}_4, \mathbf{A}_5)$, $(\mathbf{A}_5, \mathbf{A}_0)$,$(\mathbf{A}_5, \mathbf{A}_1)$, and the four unused matrix-pairs are $(\mathbf{A}_5, \mathbf{A}_2)$,$(\mathbf{A}_5, \mathbf{A}_3)$, $(\mathbf{A}_5, \mathbf{A}_4)$,$(\mathbf{A}_5, \mathbf{A}_5)$. The proposed ML detection needs to test 11 times for (11) and (12), while the original ML detection is 32 times.

This article has been accepted for publication in a future issue of this journal, but has not been fully edited. Content may change prior to final publication. Citation information: DOI 10.1109/ACCESS.2021.3095531, IEEE Access

$$(\hat{q},\hat{r}) = \begin{cases} (\tilde{q},\tilde{r}) & \text{if } m_{\tilde{q}}(t-1)+m_{\tilde{r}}(t) < m_{q'}(t-1)+m_{\tilde{l}'}(t) \\ (q',\tilde{l}') & \text{otherwise} \end{cases} \tag{14}$$

TABLE 1. The bit mapping table for Example 1.

		$\mathbf{A}(t)$					
		$\mathbf{A}_0$	$\mathbf{A}_1$	$\mathbf{A}_2$	$\mathbf{A}_3$	$\mathbf{A}_4$	$\mathbf{A}_5$
$\mathbf{A}(t-1)$	$\mathbf{A}_0$	00000	00001	00010	00011	00100	00101
	$\mathbf{A}_1$	00110	00111	01000	01001	01010	01011
	$\mathbf{A}_2$	01100	01101	01110	01111	10000	10001
	$\mathbf{A}_3$	10010	10011	10100	10101	10110	10111
	$\mathbf{A}_4$	11000	11001	11010	11011	11100	11101
	$\mathbf{A}_5$	11110	11111	X	X	X	X

Example 2: For $N_T = 4$, the original DSM has $L = 16 < 4! = 24$. In the proposed scheme, we use 9 data bits to choose 512 antenna indexes from all $24 \times 24 = 576$ permutations. Since $511 = 24 \times 21 + 7$, we have $q' = 21$ and $r' = 7$. The proposed ML detection needs to test 45 times for (11) and (12), while the original ML detection is 512 times.

Example 3: For $N_T = 5$, the original DSM has $L = 64 < 5! = 120$. In the proposed scheme, we use 13 data bits to choose 8192 antenna indexes from all 14400 permutations, and we have $q' = 68$ and $r' = 31$. The proposed ML detection needs to test 188 times for (11) and (12), much less than that for the original ML detection which is 8192 times.

In some cases, the data rate can be further increased by adding two additional bits in three blocks, e.g., $N_T = 5$ since $120^3 > 2^{20}$. The proposed mapping and detection can be easily modified for such situation.

B. BIT MAPPING BY A TABLE

For the bit mapping in Sec. III.A, if one block is detected incorrectly, perhaps most data bits of two blocks are wrong. Table 1 shows the bit mapping in Example 1 where "X" denotes an unused matrix-pair. Consider the case of $(\mathbf{A}(t-1), \mathbf{A}(t)) = (\mathbf{A}_2, \mathbf{A}_3)$. If $\mathbf{A}(t)$ is incorrectly detected and the detected values are $(\mathbf{A}_{\hat{q}}, \mathbf{A}_{\hat{r}}) = (\mathbf{A}_2, \mathbf{A}_4)$, total data bits are wrong.

In [18] and [19], we indicated that differential encoding can be performed by looking up a table. Similarly, bit mapping can be represented by a look-up table. To obtain better bit labeling for the proposed increased-rate DSM, we propose a new bit mapping that uses a look-up table. The procedure of constructing this table contains two steps. First, construct an $L \times 2L$ table which is separative bit mapping: $\log_2 L$ bits are mapped to $\mathbf{A}(t-1)$ and $\log_2 L + 1$ bits are mapped to $\mathbf{A}(t)$. Then, remove $\frac{L}{2}$ columns of $\mathbf{A}(t)$ in this table to $\frac{L}{2}$ rows of $\mathbf{A}(t-1)$. The resulting table consists of an $L \times \frac{3L}{2}$ table and an $\frac{L}{2} \times L$ table.

Take $N_T = 3$ as an example. In the first step, assume that $\mathbf{A}(t-1) \in \{\mathbf{A}_0, \mathbf{A}_1, \mathbf{A}_2, \mathbf{A}_3\}$ and $\mathbf{A}(t) \in \{\mathbf{A}_0, \mathbf{A}_1, \mathbf{A}_2, \mathbf{A}_3, \mathbf{A}_4, \mathbf{A}_5, \mathbf{A}_6, \mathbf{A}_7\}$, so two bits are mapped to $\mathbf{A}(t-1)$ and three bits are mapped to $\mathbf{A}(t)$. Table 2 shows the resulting bit mapping, for which if only one block is detected incorrectly, at most 3 data bits are wrong. Table 2 cannot be used since $\mathcal{A}'$ for $N_T = 3$ is $\{\mathbf{A}_0, \mathbf{A}_1, \cdots, \mathbf{A}_5\}$ in fact. In the second step, $\mathbf{A}_4$ and $\mathbf{A}_5$ are added to $\mathbf{A}(t-1)$ and $\mathbf{A}_6$ and $\mathbf{A}_7$ are removed from $\mathbf{A}(t)$ in Table 2. The two columns of $\mathbf{A}_6$ and $\mathbf{A}_7$ in $\mathbf{A}(t)$ are divided into two 2×2 blocks, which become two rows of $\mathbf{A}_4$ and $\mathbf{A}_5$ for $\mathbf{A}(t-1)$. One 2×2 block is removed to the two columns of $\mathbf{A}_0$ and $\mathbf{A}_1$ for $\mathbf{A}(t)$, and the other 2×2 block is removed to the two columns of $\mathbf{A}_2$ and $\mathbf{A}_3$ for $\mathbf{A}(t)$. Table 3 shows the resulting table. The 2×2 block of $\mathbf{A}_2$ and $\mathbf{A}_3$ for $\mathbf{A}(t)$ is perfect because the most right two bits of the same column are the same, but the 2×2 block of $\mathbf{A}_0$ and $\mathbf{A}_1$ for $\mathbf{A}(t)$ is imperfect. Note that switching the two 2×2 blocks has the same problem. By the same procedure, we construct bit-mapping tables for $N_T = 4$ and 5, shown in Tables 4 and 5, respectively.

To evaluate the error performance for different bit labeling, we define a parameter denoted by η which is the average number of different labeling bits in the same column or row. In Table 2, the average numbers of different labeling bits in the same column and in the same row are $(1+1+2)/3 = 4/3$ and $(1+1+1+2+2+2+3)/7 = 12/7$, respectively. Because there are totally $8 \times \binom{4}{2} = 48$ pairs for the same column and $4 \times \binom{8}{2} = 112$ pairs for the same row, its η is $(48 \times 4/3 + 112 \times 12/7)/160 = 1.6$. Although the bit mapping of Table 3 is not perfect, its η is 1.722 which is smaller than $\eta = 2.178$ in Example 1. The values of η for two bit-mapping methods are presented in Table 6 which indicates that for $N_T = 4$ and 5, the bit mapping by a table is better than the mapping in Sec. III.A.

For this bit mapping, we propose a simplified ML detection which is similar to the simplified ML detection proposed in Sec. III.A. Let

$$\tilde{q} = \arg \min_{l \in \{0,1,\cdots,L-1\}} m_l(t-1) \tag{15}$$

$$\tilde{r} = \arg \min_{l' \in \{0,1,\cdots,\frac{3L}{2}-1\}} m_{l'}(t). \tag{16}$$

$$\tilde{l} = \arg \min_{l \in \{L,L+1,\cdots,\frac{3L}{2}-1\}} m_l(t-1) \tag{17}$$

and

$$\tilde{l}' = \arg \min_{l' \in \{0,1,\cdots,L-1\}} m_{l'}(t). \tag{18}$$

and then $\mathbf{A}_{\hat{q}}$ and $\mathbf{A}_{\hat{r}}$ are determined by (19) shown on the next page. Similarly, the minimization in (18) can be obtained during the minimization in (16), so to obtain (15)-(18), only $3L < 2N_T!$ values are tested. Similar to Theorem 1, the detection by (19) is equivalent to the noncoherent ML detection. The proof is similar to the proof of Theorem 1 and thus omitted.

Simulation results for $N_T = 3$, 4 and 5 with $M = 4$ and 8 using complex-valued antenna matrices are shown in Fig. 1,

TABLE 2. The bit-mapping table in the first step for $N_T = 3$.

		$\mathbf{A}(t)$							
		$\mathbf{A}_0$	$\mathbf{A}_1$	$\mathbf{A}_2$	$\mathbf{A}_3$	$\mathbf{A}_4$	$\mathbf{A}_5$	$\mathbf{A}_6$	$\mathbf{A}_7$
$\mathbf{A}(t-1)$	$\mathbf{A}_0$	00000	00001	00010	00011	00100	00101	00110	00111
	$\mathbf{A}_1$	01000	01001	01010	01011	01100	01101	01110	01111
	$\mathbf{A}_2$	10000	10001	10010	10011	10100	10101	10110	10111
	$\mathbf{A}_3$	11000	11001	11010	11011	11100	11101	11110	11111

$$(\hat{q},\hat{r}) = \begin{cases} (\tilde{q},\tilde{r}) & \text{if } m_{\tilde{q}}(t-1)+m_{\tilde{r}}(t) < m_{\tilde{l}}(t-1)+m_{\tilde{l}'}(t) \\ (\tilde{l},\tilde{l}') & \text{otherwise} \end{cases} \tag{19}$$

TABLE 3. The proposed bit-mapping table for $N_T = 3$.

		$\mathbf{A}(t)$					
		$\mathbf{A}_0$	$\mathbf{A}_1$	$\mathbf{A}_2$	$\mathbf{A}_3$	$\mathbf{A}_4$	$\mathbf{A}_5$
$\mathbf{A}(t-1)$	$\mathbf{A}_0$	00000	00001	00010	00011	00100	00101
	$\mathbf{A}_1$	01000	01001	01010	01011	01100	01101
	$\mathbf{A}_2$	10000	10001	10010	10011	10100	10101
	$\mathbf{A}_3$	11000	11001	11010	11011	11100	11101
	$\mathbf{A}_4$	00110	00111	10110	10111		
	$\mathbf{A}_5$	01110	01111	11110	11111		

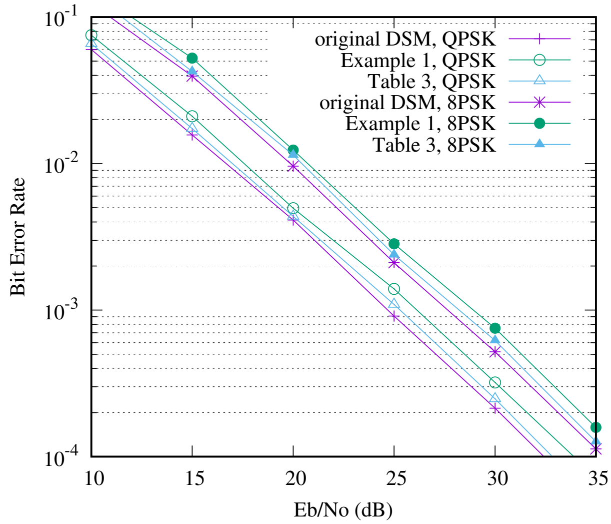

FIGURE 1. Simulation results for $N_T = 3$.

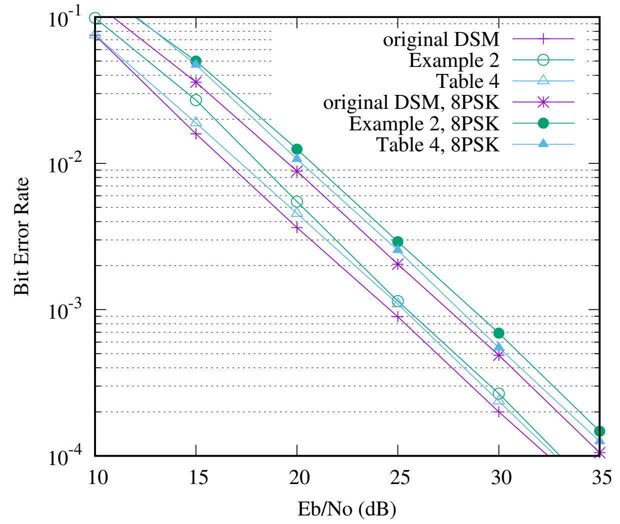

FIGURE 2. Simulation results for $N_T = 4$.

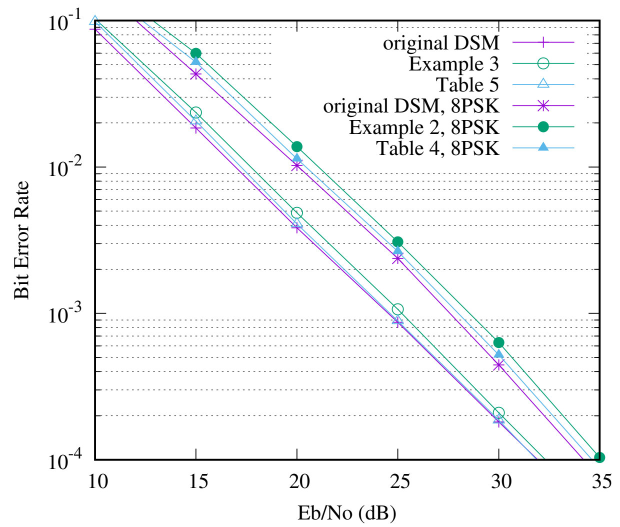

FIGURE 3. Simulation results for $N_T = 5$.

2 and 3, respectively. For all simulations in this paper, we use $N_R = 1$, and the elements in $\mathcal{A}'$ are in lexicographic order. A smaller index means a lexicographically smaller permutation. For all cases, the mapping in Sec. III.B outperforms the mapping in Sec. III.A. Compared with the original DSM, the proposed increased-rate DSM with the table mapping has higher data rates and slightly worse error performance.

IV. THE PROPOSED BC-DSM SCHEME

In the DSM scheme using repeated symbols in [6], to obtain transmitter diversity order d_T, data symbols are repeated d_T times. Consequently, only $\lfloor \frac{N_T}{d_T} \rfloor$ data symbols per block are transmitted. For example, to have $d_T = 2$ for $N_T = 4$, $\mathbf{x}(t)$ is $[x^1(t), x^1(t), x^2(t), x^2(t)]$ where $x^1(t)$ and $x^2(t)$ represent two data symbols in the tth block [6, eqn. (7)]. To increase diversity order, unlike [6] and other coded DSM schemes in [9]- [12], we propose to use BCM for $\mathcal{X}$.

TABLE 4. The proposed bit-mapping table for $N_T = 4$.

		$\mathbf{A}(t)$								
		$\mathbf{A}_0$	$\mathbf{A}_1$	$\mathbf{A}_2$	$\cdots$	$\mathbf{A}_{15}$	$\mathbf{A}_{16}$	$\mathbf{A}_{17}$	$\cdots$	$\mathbf{A}_{23}$
$\mathbf{A}(t-1)$	$\mathbf{A}_0$	000000000	000000001	000000010	$\cdots$	000001111	000010000	000010001	$\cdots$	000011000
	$\mathbf{A}_1$	000100000	000100001	000100010	$\cdots$	000101111	000110000	000110001	$\cdots$	000111000
	$\mathbf{A}_2$	001000000	001000001	001000010	$\cdots$	001001111	001010000	001010001	$\cdots$	001011000
	$\vdots$	$\vdots$	$\vdots$	$\vdots$	$\ddots$	$\vdots$	$\vdots$	$\vdots$	$\ddots$	$\vdots$
	$\mathbf{A}_{15}$	111100000	111100001	111100010	$\cdots$	111101111	111110000	111110001	$\cdots$	111111000
	$\mathbf{A}_{16}$	000011001	000011010	000011011	$\cdots$	100011111				
	$\mathbf{A}_{17}$	000111001	000111010	000111011	$\cdots$	100111111				
	$\vdots$	$\vdots$	$\vdots$	$\vdots$	$\ddots$	$\vdots$				
	$\mathbf{A}_{23}$	011111001	011111010	011111011	$\cdots$	111111111				

TABLE 5. The proposed bit-mapping table for $N_T = 5$.

		$\mathbf{A}(t)$							
		$\mathbf{A}_0$	$\mathbf{A}_1$	$\cdots$	$\mathbf{A}_{63}$	$\mathbf{A}_{64}$	$\mathbf{A}_{65}$	$\cdots$	$\mathbf{A}_{95}$
$\mathbf{A}(t-1)$	$\mathbf{A}_0$	0000000000000	0000000000001	$\cdots$	0000000111111	0000001000000	0000001000001	$\cdots$	0000001100000
	$\mathbf{A}_1$	0000010000000	0000010000001	$\cdots$	0000010111111	0000011000000	0000011000001	$\cdots$	0000011100000
	$\vdots$	$\vdots$	$\vdots$	$\ddots$	$\vdots$	$\vdots$	$\vdots$	$\ddots$	$\vdots$
	$\mathbf{A}_{63}$	1111110000000	1111110000001	$\cdots$	1111110111111	1111111000000	1111111000001	$\cdots$	1111111100000
	$\mathbf{A}_{64}$	0000001100001	0000001100010	$\cdots$	1000001111111				
	$\mathbf{A}_{65}$	0000011100001	0000011100010	$\cdots$	100001111111				
	$\vdots$	$\vdots$	$\vdots$	$\ddots$	$\vdots$				
	$\mathbf{A}_{95}$	0111111100001	0111111100010	$\cdots$	1111111111111				

TABLE 6. Comparison of η between Examples 1-3 and Tables 3-5.

	Examples 1-3	Tables 3-5
$N_T = 3$	2.178	1.722
$N_T = 4$	3.823	2.574
$N_T = 5$	5.240	3.448

Theorem 2: To achieve transmitter diversity order d_T, $\mathcal{X}$ should be a code with minimum Hamming distance $d_{\min} \geq d_T$.

Proof: Let $\mathbf{X} = \text{diag}\{\mathbf{x}\}\mathbf{A}$ and $\mathbf{X}' = \text{diag}\{\mathbf{x}'\}\mathbf{A}'$ represent two different data matrices in (3). If the minimum Hamming distance of $\mathcal{X}$ is $d_{\min} < d_T$, there are $\mathbf{x}$ and $\mathbf{x}'$ between which only $d_{\min}$ elements are different. For $\mathbf{X} \neq \mathbf{X}'$, there are only two possible cases: (i) $\mathbf{A} = \mathbf{A}'$ and $\mathbf{x} \neq \mathbf{x}'$ (ii) $\mathbf{A} \neq \mathbf{A}'$. For case (i), the different columns between $\mathbf{X}$ and $\mathbf{X}'$ is only $d_{\min}$, so the transmitter diversity is $d_{\min} < d_T$. Consequently, to achieve transmitter diversity d_T, the minimum Hamming distance of $\mathcal{X}$ should not be less than d_T. $\square$

A. BC-DSM WITH TRANSMITTER DIVERSITY ORDER 2

Let $\mathcal{X}$ be BCM whose component code is the $(N_T, N_T-1, 2)$ block code, and $\mathcal{A}$ be the systematic construction proposed in [7] with $\theta = \frac{\pi}{M}$. The received symbols can be decoded by the Viterbi algorithm. The decoding trellis diagram for an $(N_T, N_T-1, 2)$ block code needs only two states, so the overall decoding trellis diagram at the receiver needs 2^b states. Fig. 4 shows the trellis diagram for $N_T = M = 4$ where the number, say k, denotes the QPSK symbol $e^{j\frac{k\pi}{2}}$. According to (5) and (6), for $\mathbf{A}_l$, the metric of a symbol $\tilde{x}$ corresponding to $x^{(l)}_{p_l^{(k)}}(t)$ is $\sum_{i=1}^{N_R} |y_{ik}(t) - y_{ip_l^{(k)}}(t-1)\tilde{x}e^{j\theta_{l,k}}|^2$. For $\mathbf{A}_l$ where $l \in \{1, 2, \cdots, L\}$, the Viterbi decoding is done once and get a candidate $\mathbf{X}_l$ with the metric $m_l(t)$ in (6) where now $\hat{\mathbf{x}}_l(t) = [\hat{x}^{(l)}_1(t), \hat{x}^{(l)}_2(t), \cdots, \hat{x}^{(l)}_{N_T}(t)]$ is the survivor path of the trellis diagram for $\mathbf{A}_l$. The detection of $\mathbf{A}(t)$ and $\mathbf{x}(t)$ is the same as (7) and (8).

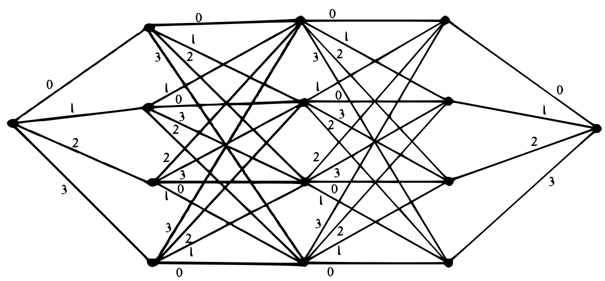

FIGURE 4. The trellis diagram for $N_T = M = 4$ where BC-DSM uses (4,3,2) component codes.

In the proposed scheme for $d_T = 2$, $\mathbf{x}(t)$ is $[x^1(t), x^2(t), \cdots, x^{N_T-1}(t), x^p(t)]$ where $x^i(t)$ is a data symbol $\forall i \in \{1, 2, \cdots, N_T-1\}$ and $x^p(t)$ is a redundant symbol due to channel coding. Therefore, the data rate of the proposed DSM with $d_T = 2$ is $[\log_2 L + b \times (N_T - 1)]/N_T$ bits/symbol. Compared with the DSM scheme using repeated symbols in [6], the proposed scheme is able to transmit additional $N_T - 1 - \lfloor \frac{N_T}{d_T} \rfloor$ data symbols per block. For $N_T = 4$ and 6, the additional data bits per block are b and $2b$ bits, respectively.

We compare BC-DSM with other coded DSM schemes for the same signal constellation of the transmitted signals. For BC-DSM, the signal constellation of the elements in $\mathbf{x}(t)$ is M-ary PSK and θ of $\mathcal{A}$ is $\frac{\pi}{M}$, so the constellation of the transmitted signals is $2M$-ary PSK. In the DSM scheme using repeated symbols in [6], the complex-valued $\mathcal{A}$ is randomly searched do the signal constellation is very complicated, so we also let $\mathcal{A}$ be the systematic construction proposed in [7] with $\theta = \frac{\pi}{M}$. Table 7 shows data rates of various coded DSM schemes, including the DSM scheme using repeated symbols, FE-DSM-DR in [9], DSTBC-ISK in [11], DSTSK-DAST in [12], DSTSK-TAST in [12] and BC-DSM, when the constellation of the transmitted signals is 8PSK or 16PSK. The data rate of FE-DSM-DR is $\log_2(Md_T)/d_T + \lfloor \log_2(N_T/d_T)\rfloor/N_T$ bits/symbol [9, eqn. (15)]. In [10], no codes with higher rates were proposed. For DSTBC-ISK, DSTSK-DAST and DSTSK-TAST, only codes for $N_T = 2$ and 4 are presented in [11] and [12]. It can be found that the data rate of BC-DSM is highest among all code DSM schemes in all four cases. Notice that other coded DSM schemes perhaps have higher diversity order than BC-DSM.

Computer simulations are done for verifying the improvement over the original full-rate DSM and the effect of complex-valued antenna-index matrices. Because other coded DSM schemes have lower data rates than the proposed scheme, their error performances are not compared with BC-DSM in simulations. Figure 5 shows simulation results of $N_T = M = 4$ where "DSM, real" denotes the full-rate DSM with real-valued antenna-index matrices whose nonzero entries are 1, "DSM, complex" denotes the original full-rate DSM using complex antenna-index matrices in [7] with $\theta = \frac{\pi}{M}$, "BC-DSM" denotes the proposed DSM, and "BC-BCM, real" denotes BC-DSM whose nonzero entries of antenna-index matrices all become 1. At high SNRs, BC-DSM outperforms other three DSMs significantly. Compared with [7] which has the same complex antenna-index matrices, BC-DSM offers more than 10 dB gain at bit error rate 10^{-4}, at the price of slight rate loss 0.5 bits/symbol.

Simulation results of $N_T = 6$ and $M = 4$ are presented in Fig. 6 where the meaning of "DSM, real" and "DSM, complex" are the same as Fig. 5, "BC-DSM (6,5,2)" represents BC-DSM using (6,5,2) component codes, and "BC-BCM (6,5,2), entries 1" denotes the BC-DSM using (6,5,2) component codes whose nonzero entries of antenna-index matrices all become 1 Still, BC-DSM has lower BER than [6] and [7], at the price of slight rate loss 0.33 bits/symbol.

B. DSM WITH TRANSMITTER DIVERSITY ORDER 3

In Theorem 2, we show that $\mathcal{X}$ with $d_{\min} \geq d_T$ is a necessary condition for DSM with transmitter diversity order d_T. If $\mathcal{A}$ is real, we will show that $\mathcal{X}$ with $d_{\min} = d_T$ and $\mathcal{A}$ with transmitter diversity order d_T is a sufficient condition for transmitter diversity order d_T.

Theorem 3: If $\mathcal{X}$ is a code with minimum Hamming distance $d_{\min} = d_T$ and $\mathcal{A}$ is real with $\min_{i\neq j} \operatorname{rank}(\mathbf{A}_i - \mathbf{A}_j) =$ d_T, then the transmitter diversity order of DSM is d_T.

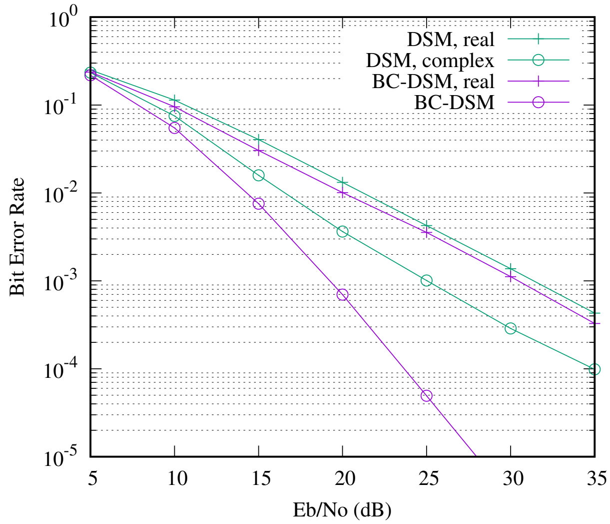

FIGURE 5. Simulation results of $N_T = M = 4$ where BC-DSM uses (4,3,2) component codes.

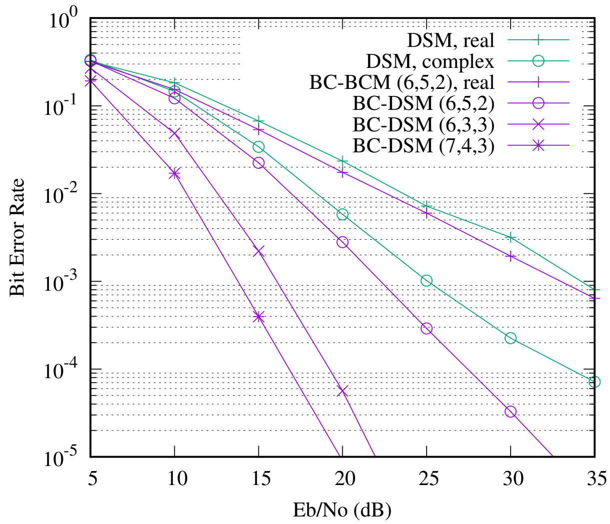

FIGURE 6. Simulation results of $M = 4$ and $N_T = 6$ or 7.

Proof: Let $\mathbf{X} = \operatorname{diag}\{\mathbf{x}\}\mathbf{A}$ and $\mathbf{X}' = \operatorname{diag}\{\mathbf{x}'\}\mathbf{A}'$ represent two different data matrices. There are two possible cases for $\mathbf{X} \neq \mathbf{X}'$: (i) $\mathbf{A} = \mathbf{A}'$ and $\mathbf{x} \neq \mathbf{x}'$ (ii) $\mathbf{A} \neq \mathbf{A}'$. For case (i), the different columns between $\mathbf{X}$ and $\mathbf{X}'$ is $d_{\min}$, so the transmitter diversity is also $d_{\min}$. For case (ii), we will show $\operatorname{rank}(\mathbf{X} - \mathbf{X}') \geq \operatorname{rank}(\mathbf{A} - \mathbf{A}')$, so the transmitter diversity is d_T.

Assume that there are d different columns (rows) between $\mathbf{A}$ and $\mathbf{A}'$. In the d columns and rows, each column and row of $\mathbf{A} - \mathbf{A}'$ contains one 1, one -1 and $N_T - 2$ zeros. Because interchanging any two columns or rows is rank-preserving,

This article has been accepted for publication in a future issue of this journal, but has not been fully edited. Content may change prior to final publication. Citation information: DOI 10.1109/ACCESS.2021.3095531, IEEE Access

TABLE 7. Data rates of various coded DSM schemes.

		DSM, repeated symbols	FE-DSM-DR	DSTBC-ISK	DSTSK-DAST	DSTSK-TAST	BC-DSM
8PSK	$N_T = 4$	2	2.25	1.25	0.75	1.25	2.5
	$N_T = 6$	2.67	2.17	–	–	–	3.17
16PSK	$N_T = 4$	2.5	2.75	1.5	1	1.5	3.25
	$N_T = 6$	3	2.67	–	–	–	4

we can permutate columns and rows of $\mathbf{A}-\mathbf{A}'$ such that

$$\mathbf{A}-\mathbf{A}' = \left(\begin{array}{cccccc|c} 1 & -1 & & & & \mathbf{0} & \\ & 1 & -1 & & & & \\ & & \ddots & \ddots & & & \\ \mathbf{0} & & & 1 & -1 & & \mathbf{0} \\ -1 & & & & 1 & & \\ \hline & & \mathbf{0} & & & & \mathbf{0} \end{array}\right). \qquad (20)$$

Obviously, the first $d-1$ columns are independent and the sum of the first d columns is zero. Hence, the rank of $\mathbf{A}-\mathbf{A}'$ is $d-1$. The corresponding $\mathbf{X}-\mathbf{X}'$ is shown on the next page. Because at least the first $d-1$ columns in (21) are independent, the rank of $\mathbf{X}-\mathbf{X}'$ is equal to or larger than $d-1$. When $\mathbf{x}=\mathbf{x}'=(1\,1\cdots1)$, $\mathbf{X}-\mathbf{X}'$ in (21) becomes $\mathbf{A}-\mathbf{A}'$ in (20), so $\min_{i\neq j}\operatorname{rank}(\mathbf{X}_i-\mathbf{X}_j)=\min_{i\neq j}\operatorname{rank}(\mathbf{A}_i-\mathbf{A}_j)=d_T$ □

In this subsection, we aim to design DSM with $d_T = 3$ for $N_T \geq 6$. As indicated in the previous subsection, the systematic construction of complex-valued antenna-index matrices proposed in [7] has $d_T = 2$ only. We randomly search complex-valued antenna-index matrices like [6], but the obtained matrices have extremely small coding gain. Note that the antenna-index matrices in [6] were random searched for the cases $N_T \leq 4$, so our unsatisfactory results are likely due to too huge search space for $N_T \geq 6$.

We propose a new method to find antenna-index matrices with a desired transmitter diversity order d_T. Unlike the methods in [6] and [7], the proposed method uses matrices whose entries are either 1 or 0. Starting from the original L antenna-index matrices, $\mathcal{A}=\{\mathbf{A}_1,\mathbf{A}_2,\cdots,\mathbf{A}_L\}$, we select matrices with transmitter diversity order d_T by the following algorithm.

Step 1 Define a set $\Phi=\mathcal{A}$ and an integer $K=L$.

Step 2 $\forall i \in \{1,2,\cdots,K\}$, compute $N_i = \sum_{j=1,j\neq i}^{K} d_{i,j}$ where $d_{i,j} = \begin{cases} 1 & \text{if } \operatorname{rank}(\mathbf{A}_i-\mathbf{A}_j) < d_T \\ 0 & \text{otherwise} \end{cases}$.

Step 3 Find $\hat{i} = \arg\max_{i\in\{1,2,\cdots,K\}} N_i$. If there are multiple values, randomly choose one. If $N_{\hat{i}}=0$, go to Step 5.

Step 4 Delete $\mathbf{A}_{\hat{i}}$ from Φ and decrease the index of $\mathbf{A}_i \forall i \in \{\hat{i}+1,\hat{i}+2,\cdots,K\}$ by 1. Decrease K by 1 and go to Step 2.

Step 5 Define $L' = 2^{\lfloor \log_2 K \rfloor}$. The set $\mathcal{A}' = \{\mathbf{A}_1,\mathbf{A}_2,\cdots,\mathbf{A}_{L'}\}$ is the used set of antenna-index matrices.

In the algorithm, N_i denotes the number of matrices which to $\mathbf{A}_i$ has diversity smaller than d_T, and removing $\mathbf{A}_{\hat{i}}$ in Step 4 can delete the most unwanted pairs whose diversity is less than d_T. This algorithm is not applied to $d_T = N_T$ since there do not exist two real matrices in $\mathcal{A}$ with full diversity. We apply the algorithm to $d_T = 3$ for $N_T = 6$ or 7. For $N_T = 6$, the obtained value of L' is 16, and the component code of BCM is the (6,3,3) block code; while for $N_T = 7$, the obtained value of L' is 64, and the component code of BCM is the (7,4,3) Hamming code. Compared with the scheme in [6], the proposed scheme is able to transmit additional one and two data symbols per block for $N_T = 6$ and 7, respectively. For $N_T = 6$ and $M = 4$, the scheme in [9] has data rate 1.167 bits/symbol, while the proposed scheme has data rate 1.667 bits/symbol. For $N_T = 7$ and $M = 4$, the proposed scheme has data rate 2 bits/symbol.

Simulation results of $d_T = 3$ with $M = 4$ are also shown in Fig. 3. For $N_T = 6$, compared with BC-DSM with $d_T = 2$, BC-DSM with $d_T = 3$ provides more than 10 dB gain at bit error rate 10^{-5}, at the price of reduced rate. For $d_T = 3$, with one more transmitter antennas, i.e., increasing $N_T = 6$ by one, the bit error rate of BC-DSM can be further improved and the data rate is increased as well.

V. CONCLUSION

In this paper, we propose two new schemes of DSM. The first scheme is able to transmit additional one bit per two blocks. For the increased-rate DSM, we propose simplified ML detection and two different bit labeling methods. With the proposed bit mapping by a table, the error performance of the proposed scheme is close to that of the original DSM. The second scheme is increased-diversity DSM called BC-DSM. With the same antenna-index matrices, BC-BCM using the $(N_T, N_T-1, 2)$ block code has transmitter diversity order $d_T = 2$ and thus outperforms the DSM in [7] significantly, at the price of only one data-symbol rate-loss. In addition, we propose an algorithm to find real-valued antenna-index matrices with a desired transmitter diversity order d_T. Compared with the coded DSM scheme in [6] and [9], the proposed BC-DSM scheme achieves higher transmission rate with the same diversity order.

REFERENCES

[1] R. Mesleh, H. Haas, S. Sinanovic, C. Ahn, and S. Yun, “Spatial modulation," *IEEE Trans. Veh. Technol.*, vol. 57, no. 4, pp. 2228-2242, Jul. 2008.

[2] J. Jeganathan, A. Ghrayeb, and L. Szczecinski, “Spatial modulation: Optimal detection and performance analysis," *IEEE Commun. Lett.*, vol. 12, no. 8, pp. 545–547, Aug. 2008.

[3] M. Wen, B. Zheng, K. J. Kim, M. D. Renzo, T. A. Tsiftsis, K.-C. Chen, and N. Al-Dhahir, “A survey on spatial modulation in emerging wireless

$$
\mathbf{X}-\mathbf{X}' = \left(\begin{array}{cccccc|ccc}
x_1 & -x_1' & & & & \mathbf{0} & & & \\
 & x_2 & -x_2' & & & & & & \\
 & & \ddots & \ddots & & & & \mathbf{0} & \\
\mathbf{0} & & & x_{d-1} & -x_{d-1}' & & & & \\
-x_d' & & & & x_d & & & & \\
\hline
 & & & & & & x_{d+1}-x_{d+1}' & & \mathbf{0} \\
 & & \mathbf{0} & & & & & \ddots & \\
 & & & & & & \mathbf{0} & & x_{N_T}-x_{N_T}'
\end{array}\right). \tag{21}
$$

systems: Research progresses and applications," *IEEE J. Select. Areas Commun.*, vol. 37, no. 9, pp. 1949–1972, Sep. 2019.

[4] Y. Cao, T. Ohtsuki, and T. Q. S. Quek, "Dual-ascent inspired transmit precoding for evolving multiple-access spatial modulation," *IEEE Trans. Commun.*, vol. 68, no. 11, pp. 6945-6961, Nov. 2020.

[5] Y. Bian, X. Cheng, M. Wen, L. Yang, H. V. Poor, and B. Jiao, "Differential spatial modulation," *IEEE Trans. Veh. Technol.*, vol. 64, no. 7, pp. 3262-3268, Jul. 2015.

[6] N. Ishikawa and S. Sugiura, "Unified differential spatial modulation," *IEEE Wireless Commun. Lett.*, vol. 3, no. 4, pp. 337-340, Aug. 2014.

[7] R. Y. Wei and T. Y. Lin, "Low-complexity differential spatial modulation," *IEEE Wireless Commun. Lett.*, vol. 8, no. 2, pp. 356-359, Apr. 2019.

[8] R. Y. Wei, "Low-complexity differential spatial modulation schemes for a lot of antennas," *IEEE Access*, vol. 8, pp. 63725-63734, 2020.

[9] R. Rajashekar, N. Ishikawa, S. Sugiura, K. V. S. Hari, and L. Hanzo, "Full-diversity dispersion matrices from algebraic field extensions for differential spatial modulation," *IEEE Trans. Veh. Technol.*, vol. 66, no. 1, pp. 385-394, Jan. 2017.

[10] R. Rajashekar, C. Xu, N. Ishikawa, S. Sugiura, K. V. S. Hari and L. Hanzo, "Algebraic differential spatial modulation is capable of approaching the performance of its coherent counterpart," *IEEE Trans. Commun.*, vol. 65, no. 10, pp. 4260-4273, Oct. 2017.

[11] C. Xu, R. Rajashekar, N. Ishikawa, S. Sugiura, and L. Hanzo, "Single-RF index shift keying aided differential space–time block coding," *IEEE Trans. Signal Process.*, vol. 66, no. 3, pp. 773-788, Feb. 2018.

[12] C. Xu, P. Zhang, R. Rajashekar, N. Ishikawa, S. Sugiura, L.Wang, and L. Hanzo, "Finite-cardinality single-RF differential space-time modulation for improving the diversity-throughput tradeoff," *IEEE Trans. Commun.*, vol. 67, no. 1, pp. 318-335, Jan. 2019.

[13] B. L. Hughes, "Differential space-time modulation," *IEEE Trans. Inform. Theory,* vol. 46, pp. 2567-2578, no. 7, Nov. 2000.

[14] B. M. Hochwald and W. Swelden, "Differential unitary space-time modulation," *IEEE Trans. Commun.,* vol. 48, pp. 2041-2052, Dec. 2000.

[15] V. Tarokh, N. Seshadri and A. R. Calderbank, "Space-time codes for high data rate wireless communication: Performance criterion and code construction," *IEEE Trans. Inform. Theory*, vol. 44, pp. 744-765, Mar. 1998.

[16] S. Sayegh, "A class of optimum block codes in signal space," *IEEE Trans. Commun.,* vol. 30, pp. 1043-1045, Oct. 1986.

[17] T. Kasami, T. Takata, T. Fujiwara and S. Lin, "On multilevel block modulation codes," *IEEE Trans. Inform. Theory,* vol. 37, pp. 965-975, July 1991.

[18] R. Y. Wei, "Differential encoding by a look-up table for quadrature-amplitude modulation," *IEEE Trans. Commun.,* vol. 59, no. 1, pp. 84-94, Jan. 2011.

[19] R. Y. Wei and L. T. Chen, "Further results on differential encoding by a table," *IEEE Trans. Commun.,* vol. 60, no. 9, pp. 2580-2590, Sep. 2012.